Tropical Gravity Wave Momentum Fluxes and Latent Heating Distributions*

MARVIN A. GELLER

Stony Brook University, Stony Brook, New York

TIEHAN ZHOU

NASA Goddard Institute for Space Studies, and Center for Climate Systems Research, Columbia University, New York, New York

PETER T. LOVE

Australian Antarctic Division, Kingston, Tasmania, Australia

(Manuscript received 17 November 2014, in final form 17 April 2015)

ABSTRACT

Recent satellite determinations of global distributions of absolute gravity wave (GW) momentum fluxes in the lower stratosphere show maxima over the summer subtropical continents and little evidence of GW momentum fluxes associated with the intertropical convergence zone (ITCZ). This seems to be at odds with parameterizations for GW momentum fluxes, where the source is a function of latent heating rates, which are largest in the region of the ITCZ in terms of monthly averages. The authors have examined global distributions of atmospheric latent heating, cloud-top-pressure altitudes, and lower-stratosphere absolute GW momentum fluxes and have found that monthly averages of the lower-stratosphere GW momentum fluxes more closely resemble the monthly mean cloud-top altitudes rather than the monthly mean rates of latent heating. These regions of highest cloud-top altitudes occur when rates of latent heating are largest on the time scale of cloud growth. This, plus previously published studies, suggests that convective sources for stratospheric GW momentum fluxes, being a function of the rate of latent heating, will require either a climate model to correctly model this rate of latent heating or some ad hoc adjustments to account for shortcomings in a climate model's land–sea differences in convective latent heating.

1. Introduction

It has long been recognized that a principal source for gravity waves (GWs) in the tropics is latent heating (e.g., Holton 1972). In recent years, there have been several efforts to incorporate meteorologically interactive GW sources in climate models. The earliest such effort to do this was in the context of incorporating a variety of meteorologically interactive GW sources by Rind et al. (1988) in a Goddard Institute for Space Studies (GISS) climate model. This was before any global observations on GW momentum fluxes were available to put observational constraints on these GW specifications. This situation has now changed, with the first comprehensive effort comparing GW momentum fluxes in climate models to those derived from observations being recently published by Geller et al. (2013). They noted several similarities and differences between the GW momentum fluxes in models and those from observations and suggested that many of these differences could be attributed to the rather crude specifications of GW sources in models.

In particular, Geller et al. (2013) noted that primary maximum absolute momentum fluxes derived from satellite observations occur at winter high latitudes while secondary maxima are located at about 20° latitude over the summer tropical continents, rather than at the latitudes of the intertropical convergence zone

* Supplemental information related to this paper is available at the Journals Online website: http://dx.doi.org/10.1175/JAS-D-15-0020.s1.

Corresponding author address: Marvin A. Geller, Stony Brook University, 111 Endeavour Hall, Stony Brook, NY 11794-5000.
E-mail: marvin.geller@sunysb.edu

DOI: 10.1175/JAS-D-15-0020.1

© 2015 American Meteorological Society

Unauthenticated | Downloaded 02/24/24 01:13 PM UTC

(ITCZ), where latent heating of the atmosphere is maximum. It is clear that wind filtering must be playing a large role in the distribution of GW momentum fluxes in the lower stratosphere since the models that had specified globally uniform GW momentum flux (GWMF) sources (HadGEM3 and MAECHAM5) and one that had a notional ITCZ GWMF source (GISS; Geller et al. 2011, their Fig. 7) show no obvious ITCZ signature, and it is also clear that both high-resolution models, CAM5 and Kanto, that seek to explicitly resolve most of the GWs, as well as the satellite observations, show strong maxima in GWMFs over the summer tropical continents, centered at about 20° latitude.

2. Tropical convection gravity wave sources: Some background

Rind et al. (1988) used a similar formulation for convectively forced GWs as they used for topographically forced GWs, but in the convective case they specified the amplitude of the convective source GWMF to be proportional to the vertically integrated cloud mass flux squared. They specified the GW phase velocities to be the vertically averaged wind over the convecting region and that wind $\pm 10\,\mathrm{m\,s^{-1}}$; however, when the convection penetrated the 400-hPa level, they launched additional GWs with a mean wind ± 20 and $\pm 40\,\mathrm{m\,s^{-1}}$. Those waves were presumed to propagate in the direction of the vertically averaged wind over the convecting region. Rind et al. (1988) used the Lindzen (1981) formalism for wave breaking in their GW parameterization, and they allowed for finite vertical propagation times by following the waves' group velocities.

Two recent efforts to develop convective GW parameterizations for use in climate models have been those of Chun and Baik (1998) and Beres (2004). Both have their GW generation as a function of latent heat released in convective systems. The Chun and Baik (1998) parameterization has been incorporated into the National Center for Atmospheric Research Community Climate Model (NCAR CCM3) by Chun et al. (2004). Their GWMFs were found to be concentrated above the ITCZ, since that was where the model latent heat release was greatest (see their Fig. 3).

Chun and her colleagues have continued development of parameterizations for the sources of convectively generated GWs since the Chun and Baik (1998) work. Song and Chun (2005) pointed out how wind shear and resonance effects can alter the distribution of cloud-top convectively generated GWMFs so that the distribution of the resulting GWMFs may not reflect the distribution of the latent heating due to these wind shear and resonance effects. Song and Chun (2008) considered the fact that GW energy propagates according to the GW group velocity, whereas almost all current GW schemes have the GW effects acting at all levels simultaneously for each model time step. A simplified version of the Song and Chun (2008) scheme, in which the GW group velocity effects (their ray-based treatment), ignoring horizontal propagation, has been implemented in the Whole Atmosphere Community Climate Model (WACCM) by Choi and Chun (2013), and their Fig. 2 shows how different the resulting GWMFs are from the latent heating distributions that are in the GW source term. This difference must arise from the wind shear and resonance effects only, since fluxes are shown at cloud-top levels in that figure.

The Beres (2004) parameterization has been implemented in the NCAR WACCM by Beres et al. (2005) and also by Richter et al. (2010). Again, their GWMFs are maximum in the ITCZ region, as may be seen in Fig. 5 in Beres et al. (2005) and Fig. 2 in Richter et al. (2010).

Thus, most recent efforts to implement GWMF sources in climate models that are consistent with the model-produced convection have specified these wave momentum flux sources to follow the latent heat release resulting from the model's subgrid-scale convective parameterizations. The exception to this is the more complicated implementation of Choi and Chun (2013), but even in that paper, there is little evidence of the GWMF maxima being centered over the summer continents at about 20° latitude, as is observed and simulated by GW-resolving models.

3. Guidance from observations

We have produced comparison plots of monthly mean rainfall rates from the TRMM satellite, which are roughly equivalent to latent heat release maps (Tao et al. 2006), cloud-top-pressure maps from the Moderate Resolution Imaging Spectroradiometer (MODIS) instrument on the *Aqua* satellite, and absolute GWMF maps from the High Resolution Dynamics Limb Sounder (HIRDLS), derived using the methods of Alexander et al. (2008) for January 2006, 2007, and 2008 and for July 2005, 2006, and 2007. Figure 1 shows these plots for January 2006, and Fig. 2 is for July 2006. The other plots are available in the electronic supplement to this paper. Given that convective rainfall over land has a much larger diurnal variation than over the ocean (e.g., Nesbitt and Zipser 2003), it is important to note the local times at which these measurements were made. TRMM has an orbit that is non sun synchronous and covers latitudes from 35°S to 35°N. Therefore, over 1 month,

Unauthenticated | Downloaded 02/24/24 01:13 PM UTC

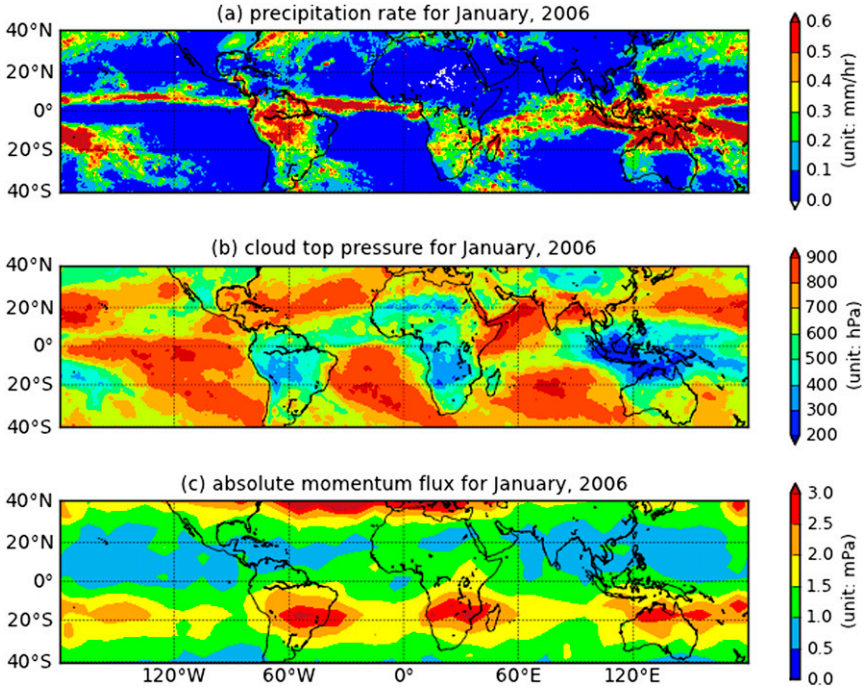

FIG. 1. (a) TRMM rainfall rates (mm h^{-1}), (b) *Aqua* MODIS cloud-top pressures (hPa), and (c) absolute gravity wave momentum flux at 20 km (mPa) derived from HIRDLS for January 2006.

TRMM data cover all local times. MODIS, on *Aqua*, has its ascending orbit equatorial time at about 1330 local time (LT). Finally, HIRDLS measurements are obtained at the equator at approximately 0100 and 1500 LT (see http://www.eos.ucar.edu/hirdls/data/products/HIRDLS-DQD_V7-1.pdf).

Looking at the HIRDLS-derived absolute momentum fluxes in both Figs. 1 and 2, one sees two regions of largest momentum fluxes. The largest absolute GWMFs are seen in a zonal band at winter high latitudes, but since we are focusing on convective forcing of GWMFs in the tropics, only a small region of large momentum fluxes are seen extending a little southward of 40°N in Fig. 1 and a bit northward of 40°S in Fig. 2, but this region of large GWMFs extends to much higher latitudes (Geller et al. 2013). Here, we focus on the secondary maxima that are seen in a zonal band in the summer hemisphere centered a bit equatorward of 20°S in Fig. 1 and at or a bit poleward of 20°N in Fig. 2, with maximum values associated with the continents at those latitudes.

Note that the rainfall rates (a proxy for the atmospheric latent heating) are maximum in the latitudinally thin regions of the ITCZ over the Atlantic and Pacific Oceans, which are slightly north of the equator in January. Other regions of significant latent heating in January are seen over the western Pacific–Indian Ocean–Indonesia–northern Australia region that bifurcates into two bands extending over the tropical Pacific Ocean a little equatorward of 10°N and between about 10° and 30°S sloping southeastward and over South America at latitudes of 0°–30°S. In July, rainfall maxima are seen over the ITCZ in the Asian monsoon regions, with weaker precipitation in a region extending from the warm pool region southeastward to about 40°S in the eastern Pacific and over the Gulf Stream and Kuroshio warm-current systems, with regions of somewhat weaker latent heating over northern South America and central Africa.

Regions of high clouds with cloud-top pressures higher than 400 hPa are seen in January around 20°S, and to a lesser extent in a band around 20°N, over South America, in a region mostly between 10° and 20°S over southern Africa and extending into the southern Indian Ocean, and in a band centered on the equator over the Indonesian warm pool region, but extending eastward over northern Australia and to the equatorial mid-Pacific region. In July, highest clouds are seen over the Asian monsoon regions and over the Himalayas, with a smaller, secondary maximum associated with the North American monsoon region, all centered at about 20°N. There are also seen somewhat lower, but still high, clouds over central Africa and over the Arabian Peninsula.

It is quite clear from Figs. 1 and 2 that the HIRDLS GWMFs more closely resemble the distribution of high

Unauthenticated | Downloaded 02/24/24 01:13 PM UTC

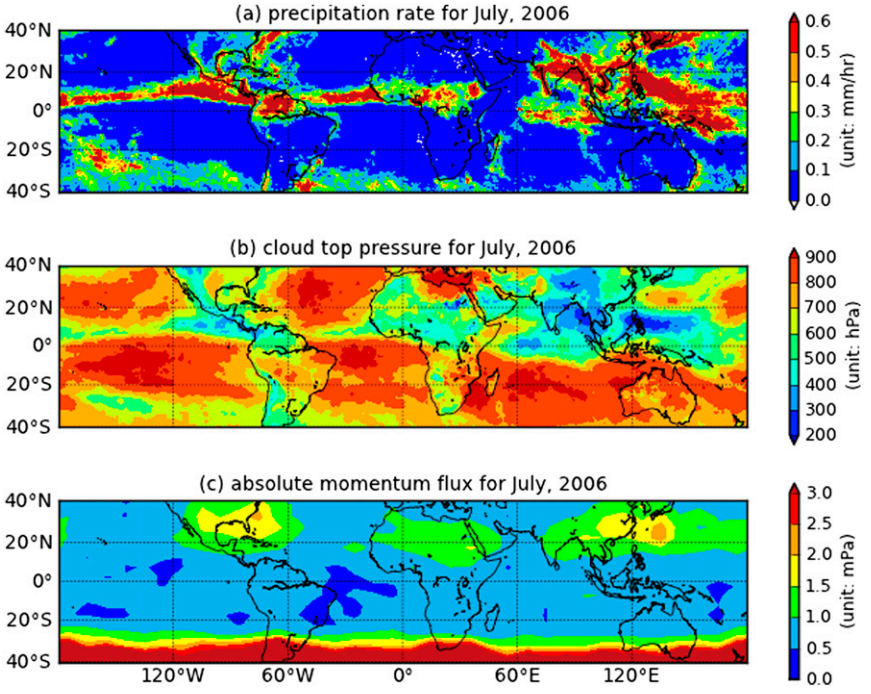

FIG. 2. As in Fig. 1, but for July 2006.

clouds (with tops higher than 400 mPa) in these January and July plots than they do the rainfall rates, which are proxies for the latent heating distributions, in that no signature is seen of the ITCZ over the oceans, for example. Of course, in most cases, the ITCZ being the exception, deep convection is also associated with intense rainfall. The cloud-top-pressure data include all cloud types, not just deep convective cloud; hence there are also some instances where high clouds are not associated with either large gravity wave momentum fluxes or high precipitation rates, such as in January over Africa at 20°N. In the following section, we look further into these comparisons.

4. Discussion of results

A first thing to note is the different local times of the rainfall rates from TRMM, the cloud-top pressures from *Aqua* MODIS, and the derived absolute GWMFs from the HIRDLS instrument on the *Aura* satellite. Nesbitt and Zipser (2003) indicate that rainfall in the tropics has a much larger diurnal variation over land (about 125% variation) than over ocean areas (about 30% variation). Moreover, this difference is even greater if one looks at very deep convective rainfall events (Liu and Zipser, 2005), where the variation is more like a factor of 13 over land and a factor of less than 2 over ocean regions.

A second thing to note is that there is abundant evidence that, despite the fact that largest rainfall rates (and latent heating) occur over the ITCZ in oceanic regions, the most active deep convection tends to occur over land areas. This has been shown by Williams and Stanfill (2002), where, among other evidence, they show that the updraft speed at all levels was greater by factors of 2–4 during the Thunderstorm Project (over land) than during GATE (over the ocean). This land–sea difference in active convection has also been shown by Liu and Zipser (2005). They showed that the seasonal variation of the occurrences of tropical convection overshooting through a reference altitude of 14 km more closely resembles the cloud-top pressures in Figs. 1b and 2b and the GWMFs in Figs. 1c and 2c than they do the precipitation rates in Figs. 1a and 2a. This is also true for the most intense precipitation features measured by TRMM, as shown by Zipser et al. (2006). Also, Cecil et al. (2005) showed that very low brightness temperatures due to strong ice scattering are about an order of magnitude larger over land than over the ocean. Finally, Kim and Alexander (2013) have shown that TRMM data show more high-frequency variability over the tropical continents than over the ITCZ, which seems consistent with the higher clouds and larger GWMFs over those continental regions.

While the results shown in this paper suggest that it is the more active convection that provides most of the

Unauthenticated | Downloaded 02/24/24 01:13 PM UTC

forcing for stratospheric GWs rather than the time-averaged latent heating, there are some technical issues related to the satellite-derived GWMFs that need to be examined. One issue is the previously mentioned diurnal variation of active convection. If the time-averaged latent heating is similar over ocean areas and over continents, as is the case in Fig. 1a over the ITCZ in the Atlantic and over northern South America, for example, the much greater diurnal variation in active convection over land than over ocean implies that the peak latent heat release over land must be greater, which in turn might imply greater lower-stratosphere GWMFs over the land area, since the rates of latent heating on the cloud time scales are greater over land areas. This can and should be checked by examining the GWMFs separately for the morning and afternoon HIRDLS measurements. One should be careful in doing this, however, since the HIRDLS team has indicated that there may be some differences between upscan and downscan results (http://www.eos.ucar.edu/hirdls/data/products/HIRDLS-DQD_V7-1.pdf). Of course, one should account for the propagation times of the GWs from their source to the lower stratosphere, but still this comparison would be interesting.

Another issue is the satellite sampling implied by the HIRDLS observational pattern (see Figs. 2.1 and 2.2 at http://www.eos.ucar.edu/hirdls/data/products/HIRDLS-DQD_V7-1.pdf). The observational sampling is more meridional in the tropics than at higher latitudes, but this difference is not great between 20°S and 20°N, so this would not seem to give rise to substantial sampling differences between these latitudes unless the GWs from the ITCZ reaching the stratosphere have much greater zonal propagation than those forced by convection over the continents. Also, Choi et al. (2012) argue that the subtropical GWs forced by convection have larger vertical and horizontal wavelengths than do the waves in deep tropics. That would make the subtropical GWMFs easier to derive from satellite observations. Another potential issue is that Bergman and Salby (1994) found that the Eliassen–Palm fluxes inferred from their satellite imagery of convection had maxima near the equator for shorter-period waves and maxima near 10°–20° for longer-period waves.

It should be noted, however, that subtropical GW activity from several satellite instruments with different diurnal coverage and wavelength sensitivities also show similar subtropical maxima. Larger GWMFs in the subtropical regions than in the tropics were also observed by the Cryogenic Infrared Spectrometers and Telescopes for the Atmosphere (CRISTA; Ern et al. 2004) and the Sounding of the Atmosphere using Broadband Emission Radiometry (SABER) instrument (Ern et al. 2011). Large temperature or radiance variances due to the GWs in the subtropics were found by the Microwave Limb Sounder (MLS; Jiang et al. 2004), the Cryogenic Limb Array Etalon Spectrometer (CLAES; Preusse and Ern 2005), and the Atmospheric Infrared Sounder (AIRS; Choi et al. 2012). Of these, MLS and AIRS focus on shorter horizontal and longer vertical wavelengths carrying larger GWMF, and both MLS and AIRS exhibit much stronger GW variances in the subtropics than in the equatorial region and no particular enhancement over the ITCZ is found. All of these instruments use different viewing geometries and local times. For instance, MLS and CLAES on the *Upper Atmosphere Research Satellite* (*UARS*) cover a whole diurnal cycle during approximately 30 days, combining ascending and descending orbit nodes. While the investigation of local time dependencies promises more insight to the forcing mechanism, the consistency of all these observations provides evidence that the contrast between tropical and subtropical GWMFs as such is neither an effect of local time nor of observation geometry. This suggests that the ''observational filter'' problem (Alexander 1998) might not be responsible for the satellite-derived subtropical maximum in GWMFs.

Finally, although the GWMFs are shown as being at an altitude of 20 km, the methodology for deriving these fluxes uses information from a much deeper layer in that this deeper layer is used to obtain the vertical wavelengths. This raises the possibility that the quasi-biennial oscillation (QBO) might be filtering out more zonally propagating waves near the equator than at 20°. This can be checked by performing simulation experiments with assumed GW spectra.

With these caveats, the results shown in Figs. 1 and 2 and also the results for additional years in the electronic supplement, taken together with the references in this section, imply that the maximum convective forcing of GWs occurs in connection with the most active, or intense, convection rather than with the maximum time-averaged latent heating.

5. Some implications

Some impressive research has shown that linear treatments for the thermal forcing of GWs from latent heat release in convective systems give a spectrum of GWs that agrees quite well with the results from fully nonlinear, cloud-resolving, mesoscale modeling of those systems [e.g., see Fig. 7 in Song and Chun (2005)] and those linear treatments have served as the basis for parameterizations of convectively forced GWs in global models (e.g., Song et al. 2007; Richter et al. 2010).

Unauthenticated | Downloaded 02/24/24 01:13 PM UTC

All of these convective treatments, however, take the velocity perturbations u' and w' to be proportional to Q, the rate of diabatic heating from latent heat release from the model's convective parameterization. Thus, the GWMF $\rho_0\overline{u'w'}$ should be proportional to $\overline{Q^2}$, where the overbar indicates averaging with time. If Q consists of its average value $\overline{Q}$ plus its fluctuations Q', then $\overline{Q^2} = \overline{Q}^2 + \overline{Q'^2}$. Now, in a climate model with GW parameterizations, the diabatic heating over a grid element will be $\overline{Q}$, where the averaging is over the area of the computational grid box and over the time step between convective physics calls.

As discussed at length in the previous section, TRMM data indicates that convection is significantly more active over the summer, tropical continents than over the ITCZ. This is manifested in higher clouds, greater updrafts, and greater higher-frequency variances in the rainfall and, thus, in the fluctuating diabatic heating.

The spectrum of convectively forced GWs has been determined by several mesoscale modeling studies and is likely well determined, but the amplitudes are more uncertain since these parameterizations are based on the thermal forcing from the climate model and information on time-varying latent heating from cloud processes and the subgrid-scale spatial variation of the latent heating is lacking in these climate models. Mesoscale models might be able to provide guidance for the adjustment of parameterizations for convectively generated GWs to adjust for the differences in the wave generation over the tropical oceans from over tropical continents, or such guidance might be obtained from the analysis of Kim and Alexander (2013) in the spatial and temporal distribution of the TRMM rainfall variances. The stochastic parameterization of Lott and Guez (2013) seems an attractive framework for incorporating this type of information for differences in GW generation over tropical oceans and continents.

It is interesting that in Choi and Chun (2013), the horizontal distribution of GWMFs differ from that of the latent heating forcing. Choi and Chun (2013) indicate that this is due to wind filtering as well as their treatment of resonance effects. Another aspect of the Choi and Chun (2013) treatment of convectively forced GWs is that they consider the finite vertical propagation times for GWs, whereas in most other GW treatments, the effects of GWs are instantaneously felt throughout the atmospheric column, corresponding to infinite GW vertical group velocities.

Finally, and perhaps most importantly, the parameterizations for convective GW sources in climate models are dependent on the results of the climate models' convective parameterizations, and these often do not produce results in agreement with observations. Dai (2006) indicates that in the 18 climate models he analyzed, there was too much (>95%) convective precipitation at most of the low latitudes relative to stratiform precipitation, whereas TRMM observations indicate that only about 45%–65% of the total precipitation is convective in these regions. He also indicates that the diurnal variation of precipitation in these models is not in good agreement with observations.

The results shown in Figs. 1 and 2, together with the cited research, suggest that the following aspects of the convection in climate models should be checked against observations: How does the ratio of convective to stratiform precipitation compare with observations? How does the land–sea contrast in deep convection compare with the observed land–sea deep convection contrast? How do the diurnal variations over land and ocean areas compare with observations?

The approximate agreement between GWMFs over the summer tropical continents and the regions of deepest convection suggest that GW forcing from convection is dominated by those regions where the rates of latent heating are largest on cloud time scales. In those regions, the clouds are highest, and the GWMFs are largest. A recent paper by Ern et al. (2014) shows good agreement between implied momentum forcing by the convergence of the absolute GWMF in the tropical stratosphere and that required to force the quasi-biennial oscillation (QBO) in the ERA-Interim. There are three issues that need to be examined here. One is that Geller et al. (2013) have shown that it is not the absolute GWMF that accelerates the mean zonal wind. Rather, it is the vector momentum flux that enters into the equations of motion. It is also shown in Geller et al. (2013) that the absolute GWMF, derived from satellite data, seems to fall off too quickly with increasing altitude. Finally, it is unclear how subtropical GWMFs leaking into the deep tropics might act to force the QBO.

Acknowledgments. This research has been supported by research grants from NASA's Earth Science Modeling and Analysis program and NSF's Climate and Large-Scale Dynamics program. We thank Dr. M. Joan Alexander for providing the satellite-derived GWMFs, and we acknowledge very useful discussions with Drs. Alexander and H.-Y. Chun. Finally, we also acknowledge three very perceptive sets of comments from anonymous reviewers.

REFERENCES

Alexander, M. J., 1998: Interpretations of observed climatological patterns in stratospheric gravity wave variance. *J. Geophys. Res.,* **103,** 8627–8640, doi:10.1029/97JD03325.

——, and Coauthors, 2008: Global estimates of gravity wave momentum flux from High Resolution Dynamics Limb Sounder

Unauthenticated | Downloaded 02/24/24 01:13 PM UTC

observations. *J. Geophys. Res.,* **113,** D15S18, doi:10.1029/2007JD008807.

Beres, J. H., 2004: Gravity wave generation by a three-dimensional thermal forcing. *J. Atmos. Sci.,* **61,** 1805–1815, doi:10.1175/1520-0469(2004)061<1805:GWGBAT>2.0.CO;2.

——, R. R. Garcia, B. A. Boville, and F. Sassi, 2005: Implementation of a gravity wave source spectrum parameterization dependent on the properties of convection in the Whole Atmosphere Community Climate Model (WACCM). *J. Geophys. Res.,* **110,** D10108, doi:10.1029/2004JD005504.

Bergman, J. W., and M. L. Salby, 1994: Equatorial wave activity derived from fluctuations in observed convection. *J. Atmos. Sci.,* **51,** 3791–3806, doi:10.1175/1520-0469(1994)051<3791:EWADFF>2.0.CO;2.

Cecil, D. J., S. J. Goodman, D. J. Boccippio, E. J. Zipser, and S. W. Nesbitt, 2005: Three years of TRMM precipitation features. Part I: Radar, radiometric, and lightning characteristics. *Mon. Wea. Rev.,* **133,** 543–566, doi:10.1175/MWR-2876.1.

Choi, H.-J., and H.-Y. Chun, 2013: Effects of convective gravity wave drag in the Southern Hemisphere winter stratosphere. *J. Atmos. Sci.,* **70,** 2120–2136, doi:10.1175/JAS-D-12-0238.1.

——, ——, J. Gong, and D. L. Wu, 2012: Comparison of gravity wave temperature variances from ray-based spectral parameterization of convective gravity wave drag with AIRS observations. *J. Geophys. Res.,* **117,** D05115, doi:10.1029/2011JD016900.

Chun, H.-Y., and J.-J. Baik, 1998: Momentum flux by thermally induced internal gravity waves and its approximation for large-scale models. *J. Atmos. Sci.,* **55,** 3299–3310, doi:10.1175/1520-0469(1998)055<3299:MFBTII>2.0.CO;2.

——, I.-S. Song, J.-J. Baik, and Y.-J. Kim, 2004: Impact of a convectively forced gravity wave drag parameterization in NCAR CCM3. *J. Climate,* **17,** 3530–3547, doi:10.1175/1520-0442(2004)017<3530:IOACFG>2.0.CO;2.

Dai, A., 2006: Precipitation characteristics in eighteen coupled climate models. *J. Climate,* **19,** 4605–4630, doi:10.1175/JCLI3884.1.

Ern, M., P. Preusse, M. J. Alexander, and C. D. Warner, 2004: Absolute values of gravity wave momentum flux derived from satellite data. *J. Geophys. Res.,* **109,** D20103, doi:10.1029/2004JD004752.

——, ——, J. C. Gille, C. L. Hepplewhite, M. G. Mlynczak, J. M. Russell III, and M. Riese, 2011: Implications for atmospheric dynamics derived from global observations of gravity wave momentum flux in stratosphere and mesosphere. *J. Geophys. Res.,* **116,** D19107, doi:10.1029/2011JD015821.

——, and Coauthors, 2014: Interaction of gravity waves with the QBO: A satellite perspective. *J. Geophys. Res. Atmos.,* **119,** 2329–2355, doi:10.1002/2013JD020731.

Geller, M. A., and Coauthors, 2011: New gravity wave treatments for GISS climate models. *J. Climate,* **24,** 3989–4002, doi:10.1175/2011JCLI4013.1.

——, and Coauthors, 2013: A comparison between gravity wave momentum fluxes in observations and climate models. *J. Climate,* **26,** 6383–6405, doi:10.1175/JCLI-D-12-00545.1.

Holton, J. R., 1972: Waves in the equatorial stratosphere generated by tropospheric heat sources. *J. Atmos. Sci.,* **29,** 368–375, doi:10.1175/1520-0469(1972)029<0368:WITESG>2.0.CO;2.

Jiang, J. H., B. Wang, K. Goya, K. Hocke, S. D. Eckermann, J. Ma, D. L. Wu, and W. G. Read, 2004: Geographical distribution and interseasonal variability of tropical deep convection: UARS MLS observations and analyses. *J. Geophys. Res.,* **109,** D030111, doi:10.1029/2003JD003756.

Kim, J.-E., and M. J. Alexander, 2013: Tropical precipitation variability and convectively coupled equatorial waves on submonthly time scales in reanalyses and TRMM. *J. Climate,* **26,** 3013–3030, doi:10.1175/JCLI-D-12-00353.1.

Lindzen, R. S., 1981: Turbulence and stress owing to gravity wave and tidal breakdown. *J. Geophys. Res.,* **86,** 9707–9714, doi:10.1029/JC086iC10p09707.

Liu, C., and E. J. Zipser, 2005: Global distribution of convection penetrating the tropical tropopause. *J. Geophys. Res.,* **110,** D23104, doi:10.1029/2005JD006063.

Lott, F., and L. Guez, 2013: A stochastic parameterization of the gravity waves due to convection and its impact on the equatorial stratosphere. *J. Geophys. Res. Atmos.,* **118,** 8897–8909, doi:10.1002/jgrd.50705.

Nesbitt, S. W., and E. J. Zipser, 2003: The diurnal cycle of rainfall and convective intensity according to three years of TRMM measurements. *J. Climate,* **16,** 1456–1475, doi:10.1175/1520-0442-16.10.1456.

Preusse, P., and M. Ern, 2005: Indication of convectively generated gravity waves observed by CLAES. *Adv. Space Res.,* **35,** 1987–1991, doi:10.1016/j.asr.2004.09.005.

Richter, J. H., F. Sassi, and R. R. Garcia, 2010: Toward a physically based gravity wave source parameterization in a general circulation model. *J. Atmos. Sci.,* **67,** 136–156, doi:10.1175/2009JAS3112.1.

Rind, D., R. Suozzo, N. K. Balachandran, A. Lacis, and G. Russell, 1988: The GISS global climate-middle atmosphere model. Part I: Model structure and climatology. *J. Atmos. Sci.,* **45,** 329–370, doi:10.1175/1520-0469(1988)045<0329:TGGCMA>2.0.CO;2.

Song, I.-S., and H.-Y. Chun, 2005: Momentum flux spectrum of convectively forced internal gravity waves and its application to gravity wave drag parameterization. Part I: Theory. *J. Atmos. Sci.,* **62,** 107–124, doi:10.1175/JAS-3363.1.

——, and ——, 2008: A Lagrangian spectral parameterization of gravity wave drag induced by cumulus convection. *J. Atmos. Sci.,* **65,** 1204–1224, doi:10.1175/2007JAS2369.1.

——, ——, R. R. Garcia, and B. A. Boville, 2007: Momentum flux spectrum of convectively forced internal gravity waves and its application to gravity wave drag parameterization. Part II: Impacts in a GCM (WACCM). *J. Atmos. Sci.,* **64,** 2286–2308, doi:10.1175/JAS3954.1.

Tao, W.-K., and Coauthors, 2006: Retrieval of latent heating from TRMM measurements. *Bull. Amer. Meteor. Soc.,* **87,** 1555–1572, doi:10.1175/BAMS-87-11-1555.

Williams, E., and S. Stanfill, 2002: The physical origin of the land–ocean contrast in lightning activity. *C. R. Phys.,* **3,** 1277–1292, doi:10.1016/S1631-0705(02)01407-X.

Zipser, E. J., D. J. Cecil, C. Liu, S. W. Nesbitt, and D. P. Yorty, 2006: Where are the most intense thunderstorms on Earth? *Bull. Amer. Meteor. Soc.,* **87,** 1057–1071, doi:10.1175/BAMS-87-8-1057.

Unauthenticated | Downloaded 02/24/24 01:13 PM UTC